THE PUBLISHING HOUSE
OF THE ROMANIAN ACADEMY

PROCEEDINGS OF THE ROMANIAN ACADEMY, Series A,
Volume 15, Number 1/2014, pp. 43–51

MODELING OF NEW SPATIAL PARALLEL STRUCTURES WITH CONSTANT PLATFORM ORIENTATION USING PLANAR PARALLEL MODULES

Calin VAIDA, Nicolae PLITEA, Dragos COCOREAN, Doina PISLA

Research Center for Industrial Robots Simulation and Testing, Technical University of Cluj-Napoca, Romania
Corresponding author: Doina PISLA, E-mail: doina.pisla@mep.utcluj.ro

The use of simple planar modules as basis in the development of innovative parallel structures leads to optimized solutions for a wide area of applications without the need of redesign. The authors propose the use of simple two degrees of freedom (DOF) modules with the actuators situated on the fixed platform for the development of a family of 3-DOF parallel mechanisms with constant platform orientation. The kinematics of each mechanism is computed along with the workspace generation emphasizing the differences which appear for different robot sizes and joint geometries. Different positioning trajectories are generated based on the kinematic model of each family of parallel mechanisms.

Key words: parallel structure, planar module, kinematics, modeling, workspace.

1. INTRODUCTION

One of the main advantages of parallel robots refer to their small masses in motion, mainly due to the multiple chains connecting the mobile platform to the base and the positioning of the actuators on the fixed platform. Many industrial applications do not require 6-DOF from the robotic system, thus, encouraging the development of simple solutions with a smaller number of degrees of freedom. The authors propose the use of planar 2-DOF modules which position all the actuators on the robot base. The different configurations are suitable for applications in various fields, from the manipulation of large masses to micro-motions.

Mourad Karouia presents in [1] a study of the kinematics of parallel spherical manipulators with 3-DOF. Another study of the kinematics is presented by Pashkevich for the 3-DOF robot named Orthoglide [2], whose kinematics behaviour is similar to the one of a Cartesian manipulator. A family of T2R1 spatial parallel manipulators with unlimited rotations is presented by Gogu in [3]. Bamberger presents in [4] the inverse kinematic model of micro parallel mechanisms with translational modules and a method for designing structures with 3, 4 and 5 passive joints. Lukanin proposed in [5] the inverse kinematic model and the determination of the workspace for a 3-SPR parallel robot. Another kinematic model is described in [6] for a 3-CRR parallel robot. Arakelian presents in [7] a new planar parallel manipulator with unlimited rotation capability, overcoming one of the major drawbacks of this type of structures. A classification of self-motions using algebraic representation of the 3-RPS is treated in [8]. Staicu describes in [9] a kinematic model of a 3-DOF parallel manipulator with prismatic active joints and proposes the Recursive Matrix Method to solve the kinematics and dynamics of all the complex manipulators [10]. Callegari presents an algorithm for solving the kinematics of an 3-RPC type parallel robot [11] and a new 3-PUU parallel mechanism whose leading translational actuators are displayed on a radial direction [12]. Zhou develops a new parallel spatial mechanism with 4 leading sliders and presents its kinematic model in [13]. Badescu studies in [14] the workspace of a 3-UPU parallel platform based on its kinematic model. Zhou presents in [15] a hybrid robot with 3-DOF composed by a parallel mechanism and a pantograph mechanism with the purpose of an increased rigidity and workspace volume. The kinematic and dynamic model is also presented in this paper. Zhao presents in [16] the kinematics of two parallel robots: 3-SPS/SP and 4-SPS/SP, used in devices for ankle rehabilitation. Yang proposes in [17] the kinematics for an 3-HSS manipulator.

The authors background in the field of 3-DOF parallel structures comprises several innovative structures: a 3-DOF spatial robot for laparoscope guidance in minimally invasive surgery [18,19], the MICABO-E planar parallel robot with flexible hinges [20], and a reconfigurable structure with 2 up to 6 DOF [21]. This paper presents some of the researches on parallel mechanisms with constant platform orientation achieved in [22], continuing their study with the modelling of their workspaces and precision mapping, kinematic comparison between different constructive variants and the kinematic modelling for speeds and accelerations for one of the proposed structures.

2. THE PLANAR 2-DOF PARALLEL MODULES

The planar 2-DOF modules enable the positioning of the characteristic point in the Oxy plane by varying the coordinates of the active joints. A first kinematic solution is illustrated in Fig. 1. The active joints 1 and 2 are positioned on a fixed frame, their actuation (through the variation of q_1 and q_2) determining the position of the characteristic point, P, in the *OXY* plane. The direct geometrical model (DGM) and the inverse geometrical model (IGM) are computed.

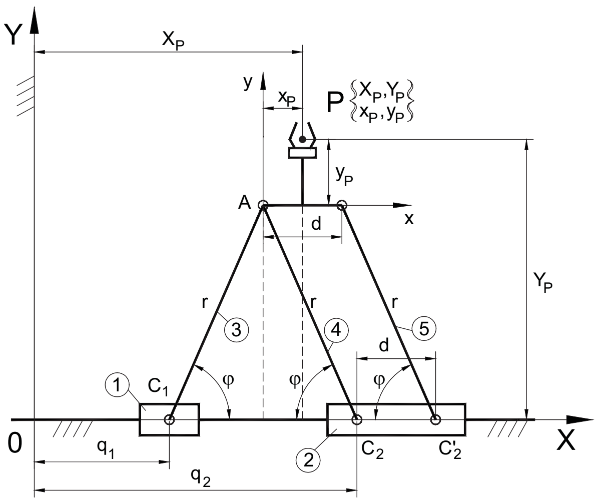

Fig. 1 – First planar 2-DOF parallel module.

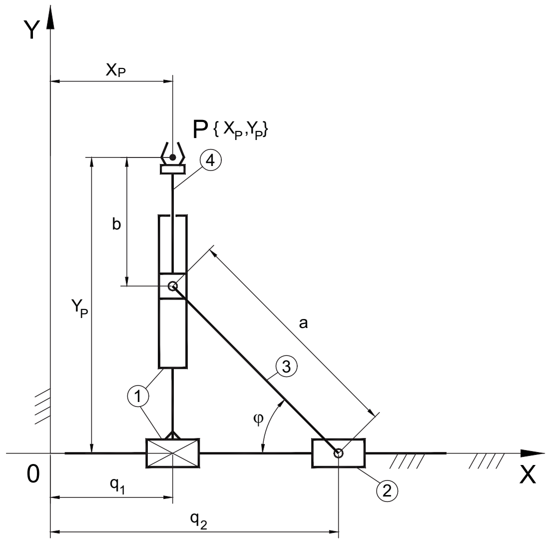

Fig. 2 – Second planar 2-DOF parallel module.

For solving the DGM the following parameters are given: q_1, q_2, d, r, x_p, y_p and the unknowns are: X_p, Y_p. From the kinematic scheme, the following equations yield:

$$\begin{cases} X_P = X_A + x_P = q_1 + r \quad c\varphi + x_P \\ Y_P = Y_A + y_P = r \quad s\varphi + y_P. \end{cases} \tag{1}$$

The angle φ can be expressed as (in all equations cos() was denoted with *c* and sin() with *s*):

$$\begin{array}{l} c\varphi = u = \dfrac{1}{2}\dfrac{q_2 - q_1}{r}; \\ s\varphi = w = \dfrac{1}{2r}\sqrt{(2r)^2 - (q_2 - q_1)^2} \end{array}, \ \varphi = \operatorname{atan2}(u, w) = \operatorname{atan2}\left[\sqrt{(2r)^2 - (q_2 - q_1)^2}, q_2 - q_1\right]. \tag{2}$$

Based on (1) and (2) the coordinates of the end-effector are:

$$\begin{cases} X_p = \dfrac{1}{2}(q_1 + q_2) + x_p \\ Y_p = \dfrac{1}{2}\sqrt{(2 \cdot r)^2 - (q_2 - q_1)^2} + y_p. \end{cases} \tag{3}$$

In order to determine the Inverse Geometrical Model (IGM), besides the geometrical parameters, d, r, x_p, y_p the coordinates of the TCP are known, namely X_p, Y_p, while the task is to determine the coordinates of the actuated joints, q_1, q_2. From equations (1) to (3) it yields:

$$q_2 = 2X_P - q_1 - 2x_P;\ \ Y_P = \frac{1}{2}\sqrt{(2r)^2 - (q_2 - q_1)^2} + y_P \text{ and } (Y_P - y_P)^2 = r^2 - \frac{(2X_P - 2q_1 - 2x_P)^2}{4}. \tag{4}$$

From (4) the expressions of the actuated joints, thus the solution for the IGM, can be written:

$$\begin{cases} q_1 = X_p - x_p - \sqrt{r^2 - (Y_p - y_p)^2} \\ q_2 = 2 \cdot X_p - q_1 - 2 \cdot x_p. \end{cases} \tag{5}$$

A second planar module is illustrated in figure 2. It preserves the same actuator characteristic as the first one, having the actuated joints, q_1 and q_2 positioned on a fixed frame. By modifying the values of the active joints, the characteristic point P can be positioned in the OXY plane.

Based on Fig. 2, using the geometrical parameters, the following equations result:

$$X_P = q_1;\quad Y_P = a \cdot s\varphi + b. \tag{6}$$

From the kinematic scheme the expression of the angle φ can be computed:

$$\begin{gathered} c\varphi = \frac{q_2 - q_1}{a};\quad s\varphi = \frac{1}{a}\sqrt{a^2 - (q_2 - q_1)^2} \quad \text{resulting that} \\ \varphi = \operatorname{atan2}\left(\sqrt{a^2 - (q_2 - q_1)^2},\ q_2 - q_1\right) \end{gathered} \tag{7}$$

Using the geometrical parameters a, b and the equations (6) and (7) the coordinates of the end-effector can be easily expressed as follows:

$$\begin{cases} X_p = q_1 \\ Y_p = b + \sqrt{a^2 - (q_2 - q_1)^2} \end{cases}. \tag{8}$$

Based on the (8) the position equations for the mechanism can be written in implicit form:

$$\begin{cases} f_1(X_P, Y_P,\ q_1, q_2) \equiv X_P - q_1 = 0 \\ f_2(X_P, Y_P, q_1, q_2) \equiv Y_P - b - \sqrt{a^2 - (q_2 - q_1)^2} = 0. \end{cases} \tag{9}$$

Based on (9) the equations of the IGM can be written as follows:

$$\begin{cases} q_1 = X_p \\ q_2 = Y_1 + \sqrt{a^2 - (X_p - b)^2} \end{cases}. \tag{10}$$

A comparison is proposed between the two modules in order to assess their particularities. Their workspace is presented along with an accuracy mapping along the workspace. In order to have a proper critical analysis, a set of parameters were defined, similar for both modules, along with a numerical set of values meant to provide quantitative data regarding their evaluation: total frame length $l = 500$ mm; normal actuator length: $l_a = 50$ mm where the length of the second actuator of module 2 is $2 \cdot l_a = 100$ mm; the actuator values range are computed taking into account that measurements are made, from their centers; the other geometrical data are equal for both modules: $y_p = d = b = 50$ mm and $r = a = 200$ mm.

Regarding the representation of the two workspaces, they represent the theoretical capabilities of the modules, as the actuators variation is forced to the limit, whereas the angle φ is varied from 0 to 90. In the same time the evaluation of the two modules accuracy with respect to a fixed increment of the actuator is performed. For both modules the variation on X axis is proportional with the actuator displacement which means that the analysis can be performed only along the X axis as along Y axis the displacement variation between two points is constant.

In order to attain an accuracy mapping of each module, the distance between two consecutive positions (dp) of the characteristic point P is compared with the increment of 1 unit for the actuators. The workspace for each module is represented now in a color scheme showing the distance between two points in different workspace areas. The value of 1 corresponds to an equal displacement variation at the level of the actuators and end-effector while values over 1 indicate a lower precision and below one better precision.

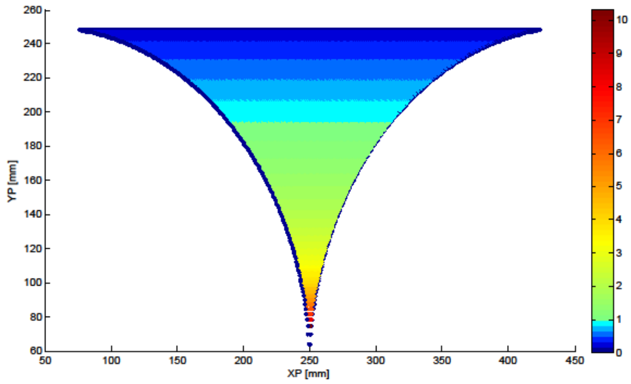

Fig. 3 – Module 1 workspace with accuracy map.

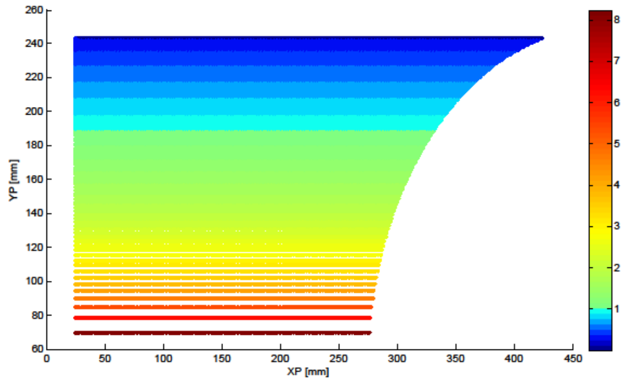

Fig. 4 – Module 2 workspace with accuracy map.

Figures 3 and 4 illustrate the workspace with accuracy mappings for each module, where the accuracy increases in accordance with the scale on the right side of each figure.

Discussion. In terms of workspace the second module provides a much wider working area but the motion accuracy is somewhat smaller. The second aspect, which is very often overlooked when analyzing kinematic schemes, refers to the type of joints used. The first module uses only rotational joints which have the same behavior for any relative position between the active joints, while the second module uses a translational joint, which tends to introduce some parasite forces when the distance between the active joints is close to the maximum possible value. This imposes careful manufacturing and the use of low friction guiding bearings. So in order to provide a definite answer regarding which module is better, a thorough application analysis is needed, as certain conditions favor any of the two modules.

3. PARALLEL MECHANISMS WITH CONSTANT PLATFORM ORIENTATION USING PLANAR MODULES

Many applications require the positioning of a given task object in space with constant or no orientation. In order to accomplish this task, a spatial structure with 3 DOF is sufficient. Thus using the planar modules two kinematic structures with all actuators positioned on the robot base are presented.

Figure 5 illustrates a solution developed using module 1, having linear actuated joints and passive rotational joints. Based on the equations (1–5) and the geometrical parameters in figure 5, the following equations can be written:

$$\begin{cases} X_P = q_1^* \\ Y_P = q_3^* \cdot c\theta_1 + a + b, \\ Z_P = h - q_3^* \cdot s\theta_1 \end{cases} \quad \begin{cases} X_P = r_2 \cdot c\theta_2 + R_2 \cdot c\varphi_2 \\ Y_P = q_2 + b \\ Z_P = h - r_2 \cdot s\theta_2 - R_2 \cdot s\varphi_2. \end{cases} \tag{11}$$

Having the geometrical parameters $d_1 = d/2, R_1, r_2, e_1, R_2$ and the given coordinates for the actuated joints q_1, q_2, q_3, the DGM has to be determined.

$$q_3^* = \frac{1}{2}\sqrt{(2R_1)^2 - (q_3 - q_1)^2} + e_1; \quad q_1^* = \frac{1}{2}(q_1 + q_3) + \frac{d}{2}; \quad \begin{cases} q_3^* \cdot c\theta_1 = Y_P - a - b \\ q_3^* \cdot s\theta_1 = h - Z_P. \end{cases} \tag{12}$$

Using (11–12) the equations for the DGM and IGM are obtained:

$$\text{DGM: }\begin{cases} X_P = q_1^* = \dfrac{1}{2}\left(q_1 + q_3\right) + \dfrac{d}{2} \\ Y_P = q_2 + b \\ Z_P = h - \sqrt{\left(q_3^*\right)^2 - \left(Y_P - a - b\right)^2} \end{cases};\quad \text{IGM: }\begin{cases} q_1 = X_P - \dfrac{d}{2} - \sqrt{R_1^2 - \left(q_3^* - y_P\right)^2} \\ q_2 = Y_P - b \\ q_3 = q_1 + 2\sqrt{R_1^2 - \left(q_3^* - y_P\right)^2} \end{cases}, \tag{13}$$

where $q_3^* = \sqrt{\left(Y_P - a - b\right)^2 + \left(h - Z_P\right)^2}$, $y_P = e_1$.

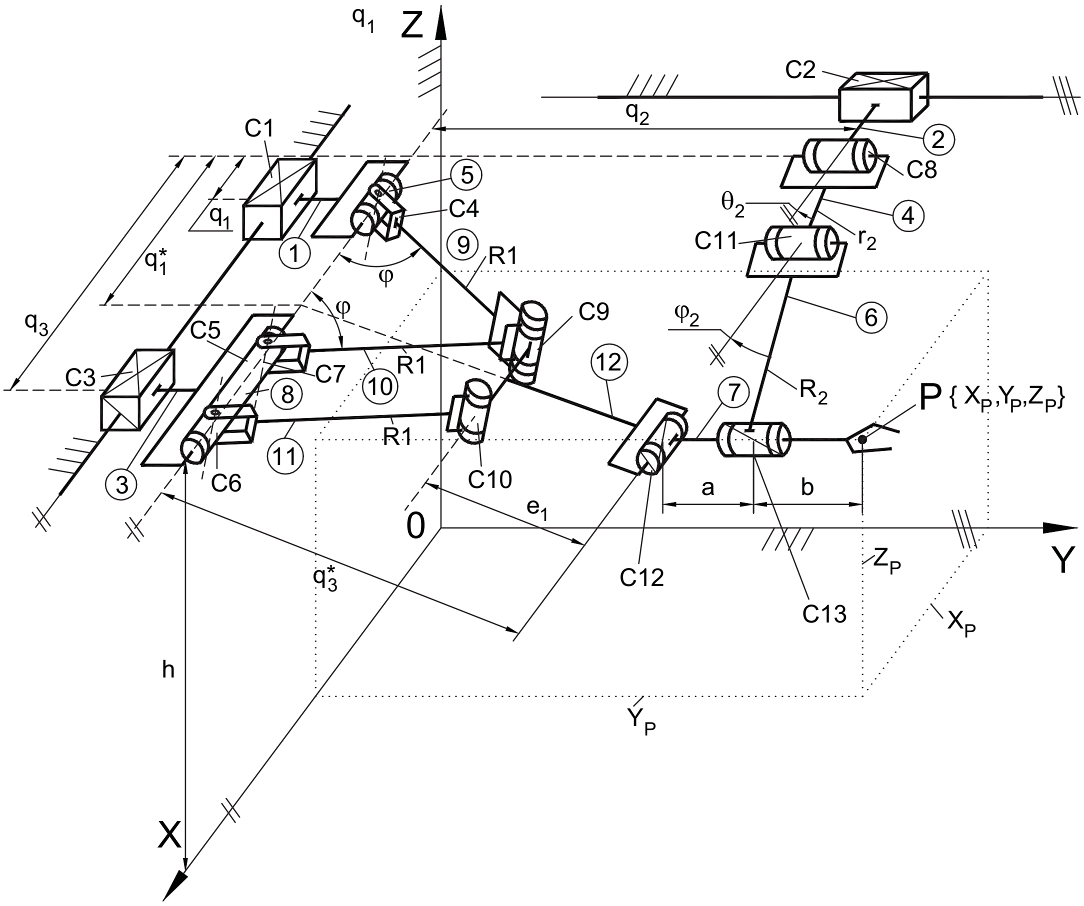

Fig. 5 – Kinematic scheme of a parallel mechanism using the first planar module.

Based on the equations (11) to (13) the implicit position equations for the mechanism:

$$\begin{cases} f_1\left(X_P, Y_P, Z_P, q_1, q_2, q_3\right) \equiv \quad X_P - \dfrac{1}{2}\left(q_1 + q_3\right) - \dfrac{d}{2} = 0 \\ f_2\left(X_P, Y_P, Z_P, q_1, q_2, q_3\right) \equiv \quad Y_P - q_2 - b = 0 \\ f_3\left(X_P, Y_P, Z_P, q_1, q_2, q_3\right) \equiv \left(Z_P - h\right)^2 - \left[\dfrac{1}{2}\sqrt{\left(2R_1\right)^2 - \left(q_3 - q_1\right)^2} + e_1\right]^2 + \left(Y_P - a - b\right)^2 = 0. \end{cases} \tag{14}$$

Another solution based on the mechanism in Fig. 2, which uses the second planar module, is presented in figure 6.

Using the equations (6–10) of the second planar module and the geometrical parameters in Fig. 6, the following equations can be written:

$$\begin{cases} X_P = q_1 \\ Y_P = (q_3^* + d_1) \cdot C\theta_1 + a + b, \\ Z_P = h - (q_3^* + d_1) \cdot S\theta_1 \end{cases} \quad \begin{cases} X_P = r_2 C\theta_2 + R_2 C\varphi \\ Y_P = q_2 + b \\ Z_P = h - r_2 S\theta_2 - R_2 S\varphi \end{cases}, \tag{15}$$

where $q_3^* = \sqrt{R_1^2 - (q_3 - q_1)^2}$.

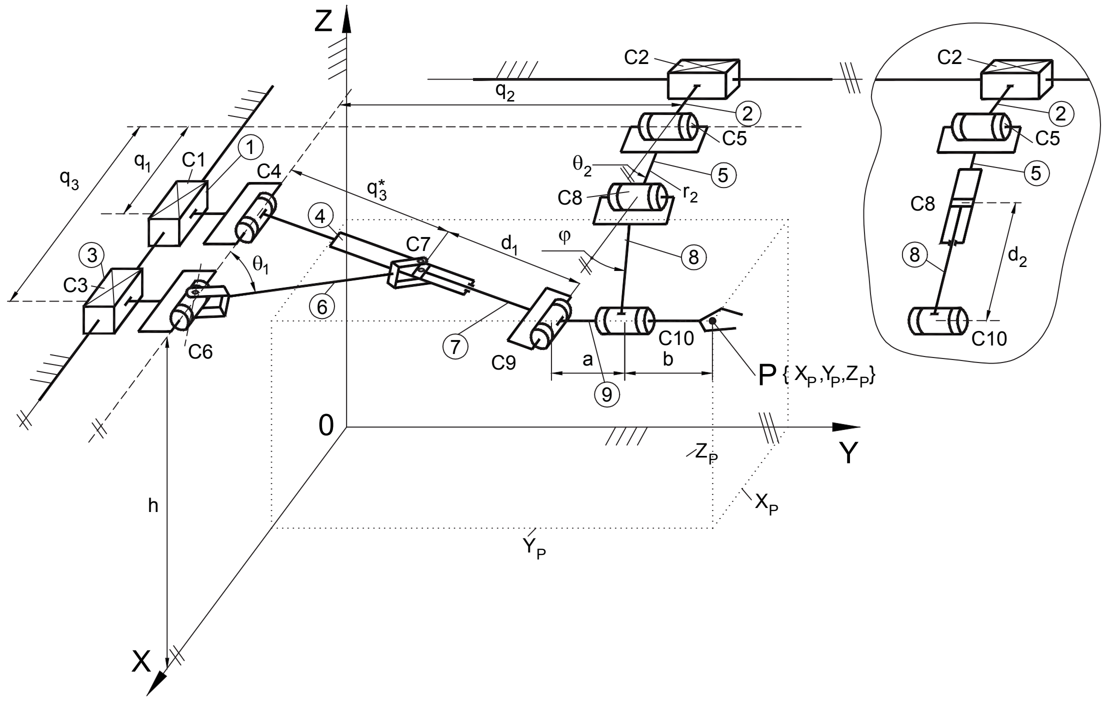

Fig. 6 – Kinematic scheme of a parallel mechanism using the second planar module.

Using (15) the equations of the DGM and IGM are obtained as follows:

$$\text{DGM: } \begin{cases} X_P = q_1 \\ Y_P = q_2 + b \\ Z_P = h - \sqrt{(q_3^* + d_1)^2 - (q_2 - a)^2} \end{cases}, \quad \text{IGM: } \begin{cases} q_1 = X_P \\ q_2 = Y_P - b \\ q_3 = X_P + \sqrt{R_1^2 - \left[\sqrt{(Y_P - a - b)^2 + (h - Z_P)^2} - d_1\right]^2} \end{cases} \tag{16}$$

Based on (15) and (16) the implicit position equations for the mechanism are:

$$\begin{cases} f_1(q_1, q_2, q_3, X_P, Y_P, Z_P) \equiv q_1 - X_P = 0 \\ f_2(q_1, q_2, q_3, X_P, Y_P, Z_P) \equiv q_2 - Y_P + b = 0 \\ f_3(q_1, q_2, q_3, X_P, Y_P, Z_P) \equiv (q_3 - q_1)^2 - R_1^2 + \left[\sqrt{(Y_P - a - b)^2 + (h - Z_P)^2} - d_1\right]^2 = 0. \end{cases} \tag{17}$$

In order to determine the expression of the θ_2 angle, from the equations (15) it results:

$$\begin{cases} R_2 \cdot C\varphi_2 = X_P - r_2 \cdot C\theta_2 \\ R_2 \cdot S\varphi_2 = (h - Z_P) - r_2 \cdot S\theta_2. \end{cases} \tag{18}$$

Thus the angles θ_2 and φ can be determined:

$$\theta_2 = \text{atan2}\left(c_2, \pm\sqrt{a_2^2 + b_2^2 - c_2^2}\right) - \text{atan2}(a_2, b_2); \quad \varphi = \text{atan2}\left(h - Z_P - r_2 S\theta_2,\ X_P - r_2 C\theta_2\right) \tag{19}$$

The mechanisms in Figs. 5 and 6 present a type I singularity when elements 5 and 8 are collinear ($\varphi = 0^\circ$) which can be eliminated by replacing the revolute joint C8 with a translational joint, as it is shown in the right side of Fig. 6. A workspace comparison has been made for the two solutions of the mechanism in Fig. 6, which differ by a passive joint, namely C8 which is firstly a revolute joint and secondly a translational one. Figures 7 and 8 show the comparative workspaces for the two solutions of the mechanism, where the same dimensional properties have been used.

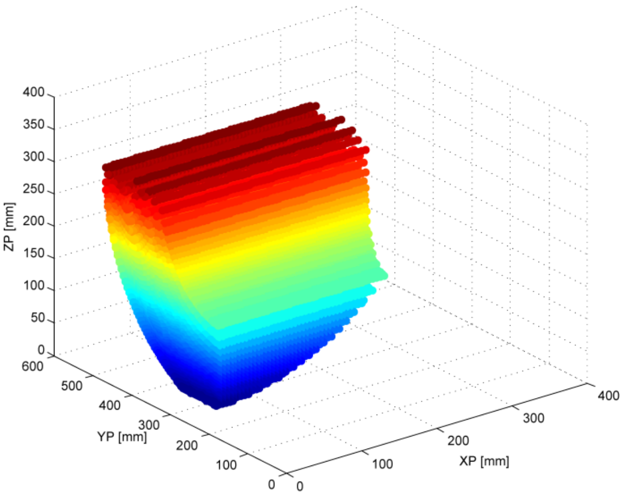

Fig. 7 – Workspace of the parallel mechanism using the C8 as rotational joint.

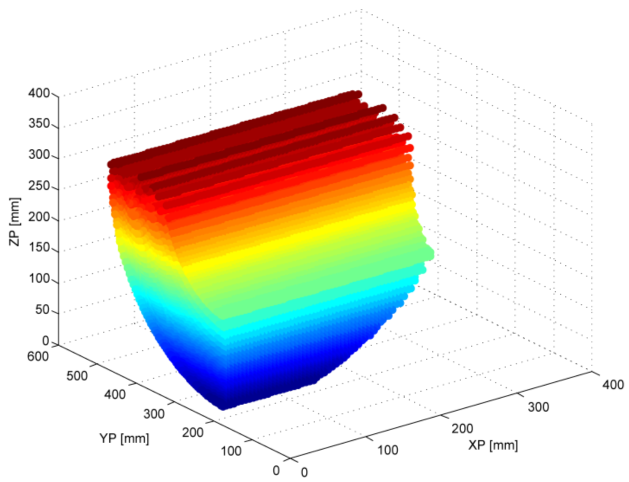

Fig. 8 – Workspace of the parallel mechanism using the C8 as translational joint.

The workspace gain, for the mechanism with the translational C8 joint is 32.97%, but as a drawback the higher friction forces must be taken into account. Again, depending on the application, one or the other mechanism might prove better. For example in a scenario where workspace size is very important and the overall accelerations are low, the solution using the translational joint is clearly better, while in a scenario where accelerations must be very high (over 1 g) the mechanism with the C8 revolute joint is more suitable.

4. SIMULATION RESULTS

The algorithms presented in the paper have been implemented in MATLAB and the simulation results for two structures are presented. Having solved the IGM and DGM for each structure together with the implicit functions which enable the determination of the Jacobi matrices, the MATLAB algorithm contains also the equations for speeds and accelerations, obtained by solving the inverse kinematical model, based on the well-known equations [23]:

$$\dot{q} = -B^{-1} A \dot{X}\ ; \quad \ddot{q} = -B^{-1}\left(A\ddot{X} + \dot{A}\dot{X} + \dot{B}\dot{q}\right), \tag{20}$$

where A and B are the Jacobi matrices.

The 3-DOF mechanism selected for the simulation is presented in figure 9. The selected geometrical parameters, expressed in millimetres are: $d_1 = 137$, $d_2 = 145$, $a = b = 60$, $r_1 = 315$, $h = 325$. In the simulation the robot achieved a linear trajectory in space, between two points having the initial and final coordinates, as presented in Fig. 9: $X_i = 245$ mm; $Y_i = 400.84$ mm; $Z_i = 121.49$ mm; and $X_f = 280$ mm; $Y_f = 370$ mm; $Z_f = 140$ mm.

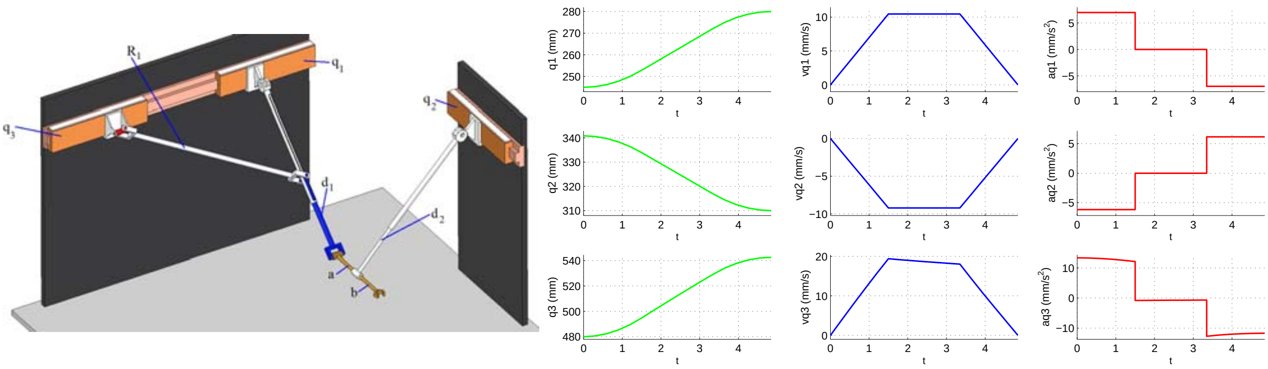

Fig. 9 – Simulation results for a linear trajectory in space achieved by the 3-DOF parallel robot with constant orientation.

5. CONCLUSIONS

In this paper the kinematic modelling of new spatial parallel structures with constant platform orientation are presented. The structures have been developed using simple 2-DOF planar modules in different configurations which cover a large area of applications. Starting with the modelling of the planar modules, several innovative 3-DOF special structures have been proposed. Workspace analysis for different configurations was computed and simulation results were presented, in terms of displacements, speeds and accelerations at the level of the actuated joints for a given spatial trajectory. These structures can be used as modules in the construction of modular parallel robots for minimally invasive medical applications.

ACKNOWLEDGEMENTS

This paper was supported by the project no. 173/2012, code PN-II-PCCA-2011-3.2-0414, entitled „Robotic assisted brachytherapy, an innovative approach of inoperable cancers – CHANCE", the bilateral project Romania – Slovenia, nr. 528/2012, "Simulation and control techniques for robots used in minimally invasive surgery" both financed by UEFISCDI and the Scopes International Grant IZ74Z0-137361/1, Creative Alliance in Research and Education focused on Medical and Service Robotics.

REFERENCES

1. MOURAD K. AND HERVE J.M., *Non-overconstrained 3-DOF spherical parallel manipulators of type: 3-RCC, 3-CCR, 3-CRC*, Robotica, **24**, pp. 85–94, 2006.
2. PASHKEVICH A., CHABLAT D., WENGER P., *Kinematics and Workspace analysis of a three-axis parallel manipulator: The Orthoglide*, Robotica, **24**, pp. 39–49, 2006.
3. GOGU, G., *A New Family of Maximally Regular T2R1-type Spatial Parallel Manipulators with Unlimited Rotation of the Moving Platform*, Proc. of ACRA, Canbera, Australia, 3–5 December, 2008.
4. BAMBERGER H., WOLF A., SHOHAM M., *Architecture of Translational Parallel Mechanism for MEMS Fabrication*, 12th IFToMM World Congress, Besancon (France), June 18–21, 2007.
5. LUKANIN V., *Inverse kinematics, forward kinematics and working space determination of 3DOF parallel manipulator with S-P-R joint structure*, Periodica Politechnica Ser. Mech. Eng., **49**, *1*, pp. 39–61, 2005.
6. XIANWEN K., GOSSELIN C.M., *Kinematics and Singularity Analysis of a Novel Type of 3-CRR 3-DOF Translational Paralel Manipulator*, The International Journal of Robotics Research, **21**, *9*, pp. 791–792, 2002.
7. ARAKELIAN V., BRIOT S., YATSUN S., YATSUN A., *A New 3-DoF Planar Parallel Manipulator with Unlimited Rotation Capability*, 13th World Congress in Mechanism and Machine Science, Guanajuato, México, 19–25 June, 2011.
8. HUSTY, M., SCHADLBAUER, J., CARO, S., WENGER, P., *Self-Motions of 3-RPS Manipulators*. New Trends in Mechanism and Machine Science, Theory and Application in Engineering, Springer-Verlag, 2012, pp. 121–130.
9. STAICU, S., *Inverse dynamics of the spatial 3-RPS parallel robot*, Proc. of the Romanian Academy, **13**, *1*, pp. 62–70, 2012.
10. STAICU S., ZHANG D., RUGESCU R. *Dynamic modeling of a 3-DOF parallel manipulator using recursive matrix relations*, Robotica, **24**, pp. 125–130, 2006.
11. CALLEGARI M., TARANTINI M., *Kinematic Analysis of Novel Translation Platform*, J. Mech. Des., **125**, *2*, 308–315, 2003.

12. CALLEGARI M., MARZETTI P. *Kinematic Characterization of a 3-PUU Parallel Robot*, Proc. Intelligent Manipulation and Grasping: IMG04, Genova, Italy, 2004, pp. 377–382.
13. ZHOU, K., MAO, D., TAO, Z., *Kinematic Analysis and Application Research on a High-Speed Travelling Double Four-Rod Spatial Parallel Mechanism*, Int. J. Adv. Manuf. Technol., **19**, pp.873–878, 2002.
14. BADESCU, M., MORMAN, J., MAVROIDIS, C., *Workspace optimization of 3-UPU parallel platforms with joint constraints*, Robotics and Automation, **4**, pp. 3678–3683, 2002.
15. ZHOU B., XU Y., *Robust control of a 3-DOF hybrid robot manipulator*, Int. J. Adv. Manuf. Technol., **3**, pp. 604–613, 2007.
16. ZHAO T., DAI J. S., NESTER C., *Sprained Ankle Physiotherapy Based Mechanism Synthesis and Stiffness Analysis of a Robotic Rehabilitation Device*, Autonomous Robots, **16**, pp. 207–218, 2004.
17. YANG Z.-Y., WU J., HUANG T., NI Y.-B., *Kinematic Model Building and Servo Parameter Identification of 3-HSS Parallel Mechanism*, Front. Mech. Eng. China, **1**, pp. 60–66, 2, 2006.
18. PISLA D., PLITEA N., VAIDA C., *Kinematic Modelling and Workspace Generation for a New Parallel Robot Used in Minimally invasive Surgery*, Advances in Robot Kinematics, 2008, pp. 459–469.
19. PISLA D., et al., *PARAMIS parallel robot for laparoscopic surgery,* Chirurgia, **105**, *5*, pp. 677–683, 2010.
20. RAATZ, A., et al., *Design and Modeling of Compliant High-Precision Parallel Robots*, PKS 2006, Chemnitz, Germany.
21. PLITEA N., LESE D., PISLA D., VAIDA C., *Structural design and kinematics of a new parallel reconfigurable robot*, Robotics and CIM, **29**, *1*, pp. 219–235, 2013
22. PISLA, D., et al., *Kinematics of new parallel structures with 3 and 4 DOF using planar parallel modules*, Proceedings of the 13th World Congress in Mechanism and Machine Science, Guanajuato, Mexico, 19–25 June 2011, pp. 1–9, A7–543.
23. MERLET J.-P., *Parallel robots*, Second Edition, 2006.

Received May 1, 2013